Journal of Physiology (1990), **430**, *pp.* 273–295
With 12 figures
Printed in Great Britain

MULTIPLE ACTIONS OF PINACIDIL ON ADENOSINE TRIPHOSPHATE-SENSITIVE POTASSIUM CHANNELS IN GUINEA-PIG VENTRICULAR MYOCYTES

BY ZHENG FAN, KEIKO NAKAYAMA* AND MASAYASU HIRAOKA

*From the Department of Cardiovascular Diseases, Medical Research Institute and * 2nd Department of Internal Medicine, Tokyo Medical and Dental University, 1-5-45 Yushima, Bunkyo-ku, Tokyo 113, Japan*

(*Received 9 November 1989*)

SUMMARY

1. The patch-clamp method was used to study the effects of pinacidil on the adenosine 5′-triphosphate (ATP)-sensitive K^+ channel current in guinea-pig ventricular myocytes.

2. In the inside-out configuration of the patch membranes, the channel activity revealed a nearly fully open state in the absence of ATP, whereas application of ATP (0·1–5 mM) markedly suppressed the channel opening. Addition of pinacidil (0·02–1·0 mM) antagonized the inhibitory action of ATP and induced channel opening without marked change in conductance. An increase in ATP concentration depressed the maximal effect of pinacidil. Consequently, the dose–response relationship of ATP inhibition was shifted to the right, but the shift approached a limiting value as pinacidil concentration was increased. The results indicate that the antagonism between pinacidil and ATP is not competitive.

3. The dose–response curve for activation of the channel by pinacidil examined at −50 mV showed a sigmoidal shape but at +50 mV it had a convex shape, revealing asymmetry in the activating effects of pinacidil at these two voltages.

4. In the absence of ATP, pinacidil produced a voltage-dependent block at positive voltages by decreasing the mean open time and increasing the mean closed time, whereas no such effects were observed at negative voltages. The concentration–block relation at a given voltage was fitted to a first-order Hill saturation function. The K_d (dissociation constant) decreased with depolarization from 2·2 mM at +20 mV to 0·15 mM at +80 mV.

5. The kinetics of block and unblock by pinacidil were shown to be slow, and were expressed by a first-order transition model. The blocking and unblocking rate constants were voltage dependent.

6. The slow block of single-channel current showed an exponential decay in the ensemble current. The time constant of the decay was voltage dependent, reaching a maximal value at around +50 mV.

7. In the absence of ATP, the channel activity gradually decreased and eventually stopped within 12–20 min, a process known as run-down of channel activity. Calcium accelerated this run-down process. Application of pinacidil partially reactivated the

channel. Such channel reactivation by pinacidil during the course of run-down depended upon the conditions of the patch and the time course of the run-down. Pre-treatment of the channel with ATP markedly strengthened the reactivation effect of pinacidil.

8. These results indicate that there are multiple sites or processes for interaction of pinacidil with the ATP-sensitive K^+ channel.

INTRODUCTION

The existence and properties of the adenosine 5′-triphosphate (ATP)-sensitive K^+ channel have been described in the membranes of cardiac muscle cells (Noma, 1983; Kakei & Noma, 1984; Trube & Hescheler, 1984), skeletal muscle cells (Spruce, Standen & Stanfield, 1985, 1987), pancreatic β-cells (Cook & Hales, 1984; Findlay, Dunne & Petersen, 1985; Rorsman & Trube, 1985) and recently in arterial smooth muscle cells (Standen, Quayle, Davies, Brayden, Huang & Nelson, 1989). Because of its wide distribution in various tissues and possible physiological importance (see Ashcroft, 1988), increasing efforts have been made to clarify the function and regulatory mechanism of this ion channel. Recently, it was found that pinacidil ((±)-*N*-cyano-4-pyridyl-*N*-1,2,2-trimethylpropylguanidine monohydrate) activates the ATP-sensitive K^+ channel in cardiac cells (Escande, Thuringer, LeGuern, Courteix, Laville & Cavero, 1989; Arena & Kass, 1989; Fan, Nakayama & Hiraoka, 1990) and in smooth muscle cells (Standen *et al.* 1989), although its precise mechanism has not been clarified. To understand further the action of pinacidil on the ATP-sensitive K^+ channel, we performed patch-clamp experiments using cell-free and cell-attached membranes of guinea-pig ventricular myocytes.

METHODS

Preparation

Single ventricular myocytes were isolated from guinea-pig hearts by enzymatic dissociation, as described previously (Hirano & Hiraoka, 1988). Briefly, the animals were anaesthetized with pentobarbitone sodium (40–50 mg/kg) after heparin administration (300 i.u./kg). The chest was opened under artificial respiration and the aorta was cannulated before removal of the heart. Using a Langendorff apparatus, the excised heart was first perfused with Tyrode solution and then with low-Ca^{2+} Tyrode solution containing 0·04% collagenase (type I, Sigma Chemical Company, St Louis, MO, USA). The temperature of all perfusates was kept at 36–37 °C during coronary perfusion. The heart was then stored in high-K^+, low-Cl^- solution (Isenberg & Klöckner, 1982) at room temperature for 60 min. Single cells were obtained by gentle agitation of small pieces of ventricular tissue in a beaker containing the high-K^+, low-Cl^- solution. The preparations were then transferred to a recording chamber placed on the stage of an inverted phase-contrast microscope (Diaphot TMD, Nikon Co., Tokyo). A single isolated cell having a smooth surface with clear striations was then selected for electrical measurement as described below. All the experiments were performed in the inside-out patch configuration in either the cell-free or open-cell modes (Kakei, Noma & Shibasak, 1985), as indicated in the text.

Solutions

The Tyrode solution contained (mM): NaCl, 143; KCl, 4; $MgCl_2$, 0·5; $CaCl_2$, 1·8; NaH_2PO_4, 0·33; glucose, 5·5; HEPES, 5. The low-Ca^{2+} Tyrode solution contained 0·03 mM-$CaCl_2$, with other components the same as in the Tyrode solution. The high-K^+, low-Cl^- solution contained (mM): glutamic acid, 70; taurine, 15; KCl, 30; KH_2PO_4, 10; HEPES, 10; MgCl, 0·5; glucose, 11; EGTA, 0·5; the pH was adjusted to 7·3–7·4 with KOH. The bathing solution (artificial intracellular

medium, ATP free) contained (mM): KCl, 142; HEPES, 5; EGTA, 2; glucose, 5·5; the pH was adjusted to 7·3–7·4 with KOH. When K_2ATP was added into the solution, the final K^+ concentration was maintained constant at 142 mM by varying KCl. Assuming that residual concentrations of Ca^{2+} and Mg^{2+} in the solution were nominally zero, free Ca^{2+} and Mg^{2+} were estimated at least less than 2×10^{-10} M and 5×10^{-6} M, respectively, in the ATP-free solution, and they were less than 2×10^{-10} M and 2×10^{-7} M, respectively, in 2 mM-ATP solution, from the apparent dissociation constants (Fabiato & Fabiato, 1979). In the case of Ca^{2+}-containing solution, EGTA was replaced by 1·0 mM-$CaCl_2$. The pipette solution (extracellular medium) contained (mM): KCl, 140; $CaCl_2$, 1·8; $MgCl_2$, 0·53; HEPES, 5; glucose, 5·5; the pH was adjusted to 7·3–7·4 with KOH. Pinacidil was dissolved in 0·05 M-HCl to make a fresh stock solution on each experimental day and diluted appropriately before use. After addition of pinacidil to the perfusate, the pH was re-adjusted to 7·3–7·4 with KOH. Pinacidil was a gift from Shionogi Pharmaceutical Co., Osaka.

The bath solution could be replaced completely within 30 s by switching from one solution to another. Experiments were done at a room temperature of 22–25 °C.

Recording methods

The patch-clamp technique (Hamill, Marty, Neher, Sakmann & Sigworth, 1981) was applied to record the current through single channels using a patch-clamp amplifier (Axopatch, Axon Inst. Inc., Burlingame, CA, USA). The current signals were amplified to 0·2 V/pA and then stored on a video cassette recorder (HR-S 7000, Victor Co., Tokyo) via a PCM converter system (RP-882, NF Inst., Yokohama) at a conversion rate of 40 kHz. The recorded signals were filtered off-line through an 8-pole Bessel low-pass filter (48 dB/octave, FV-665, NF Inst., Yokohama) at a −3 dB frequency (f_c) and digitized at 5–30 kHz onto the disc of a computer (IBM-PC/AT) using an analog-to-digital converter (CED 502, Cambridge Electronic Design Ltd, Cambridge, UK). In experiments where step potentials were applied to the patch membrane, deviation caused by the leak resistance was compensated by adding an analog current pulse to the output of the signal. The capacitive currents were minimized by adjusting the series resistance compensation and capacity compensation of the amplifier. Complete removal of capacity and leakage currents was done digitally by averaging sweeps that contained no channel openings, which were obtained by raising the intracellular ATP concentration to 5 mM, or after run-down of the channel.

Data analysis

A '50% threshold' criterion was used to detect events with the help of manual confirmation. Open and closed times were measured from records where only a single channel was active. Each distribution histogram of open or closed time was formed from continuous recordings of more than 120 s. A simplex method of least-squares analysis (Nelder & Mead, 1965) was applied for fitting a probability density function with a form of single or double exponentials of open or closed times. In order to increase the number of observations, an overall estimate of mean open time was also applied to the records from multiple-channel patches (Fenwick, Marty & Neher, 1982).

The open probability (P_o) was calculated using the equation derived by Spruce *et al.* (1985):

$$P_o = (\sum_{j=1}^{N} t_j j)/(T_d N), \quad (1)$$

where t_j is the time spent at current levels corresponding to $j = 0, 1, 2, \ldots N$ channels in the open state. T_d is the duration of the recording and N is the number of channels active in the patch. Recordings of 10–60 s were required for measurement of P_o; the longer times were required for greater N. In the early experiments, when more than one channel was active in a patch, we estimated N by means of the maximum-likelihood method (Patlak & Horn, 1982; Standen, Stanfield & Ward, 1985). The estimated N was not different from that derived by inspection of the record in ATP-free solution at positive potentials where P_o was around 1·0.

Data are presented as mean ± S.E.M. Student's unpaired t test was used to calculate statistical significance. A P value of less than 0·05 was considered significant.

Measurement of properties of ATP-sensitive K^+ channels in inside-out patches

After a patch membrane was isolated from the cell in the ATP-free solution, the ATP-sensitive K^+ channel immediately became active, reaching a maximal P_o. The P_o was not very sensitive to changes in the membrane potential, except at negative voltages, because of the fast-flickering

nature of the channel. In our experiments, within 3 min of patch excision the values of P_o were $0{\cdot}99 \pm 0{\cdot}01$ ($n = 32$) and $0{\cdot}79 \pm 0{\cdot}02$ ($n = 35$) at holding potentials of +50 and −50 mV, respectively. The P_o then declined progressively, a process referred to as channel 'run-down'. We found, however, that about 10% of the 130 patches were able to maintain nearly a constant activity for

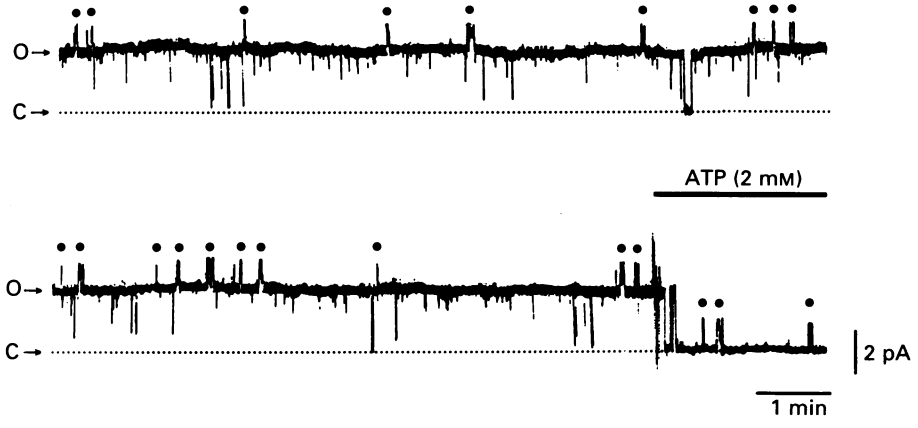

Fig. 1. An example of long survival of an ATP-sensitive K^+ channel in ATP-free solution. The chart recording was made from a cell-free inside-out patch during continuous perfusion with ATP-free bathing solution. $V_m = +50$ mV. There are two active channels with different conductances in this patch. The one with the larger conductance remained open during nearly all of the recording. This channel is identified as an ATP-sensitive K^+ channel because in the final part of the recording it is closed after addition of 2 mM-ATP to the bathing solution, whereas the smaller channel (●) remained active. C, closed level; O, open level for the ATP-sensitive K^+ channel in this and following figures. An outward current is upward and an inward current downward. The current records were filtered at $f_c = 0{\cdot}5$ kHz for display.

more than 10 min. Figure 1 shows one example of such patches. The membrane potential was held at +50 mV. In this patch, apparently two different channels can be identified and both survived in ATP-free solution for as long as 20 min. The channel having the larger current amplitude was recognized as an ATP-sensitive K^+ channel since application of 2 mM-ATP quickly suppressed its activity, while the channel with the smaller current amplitude remained active. The data from the experiments on patches with maintained activity were collected to confirm the effects of pinacidil on the channel in the absence of run-down. In order to avoid the distortion of statistically summarized results from run-down, experiments on patches that exhibited tendency to run-down were performed within 5 min after excision. After the experimental protocol was completed, the channel activity was again checked in ATP-free solution to confirm that the P_o value was not less than 90% of that immediately after the excision; otherwise the experiment was discarded from the data analysis.

RESULTS

Activation of ATP-sensitive K^+ current by pinacidil

Pinacidil activates the ATP-sensitive K^+ channel in the presence of ATP

In the presence of ATP, addition of pinacidil to the bath solution was able to activate the ATP-sensitive K^+ channel. Figure 2 shows single-channel current records during the application of ATP and pinacidil in a patch containing only one active channel at potentials of +50 and −50 mV. In the absence of ATP and

pinacidil, the channel opened almost all of the time at both potentials. When 1 mM-ATP was applied to the internal face of the patch membrane, the channel reverted to the closed level with only brief openings. Successive increases in pinacidil concentration gradually activated the ATP-sensitive K^+ channel, by increasing the

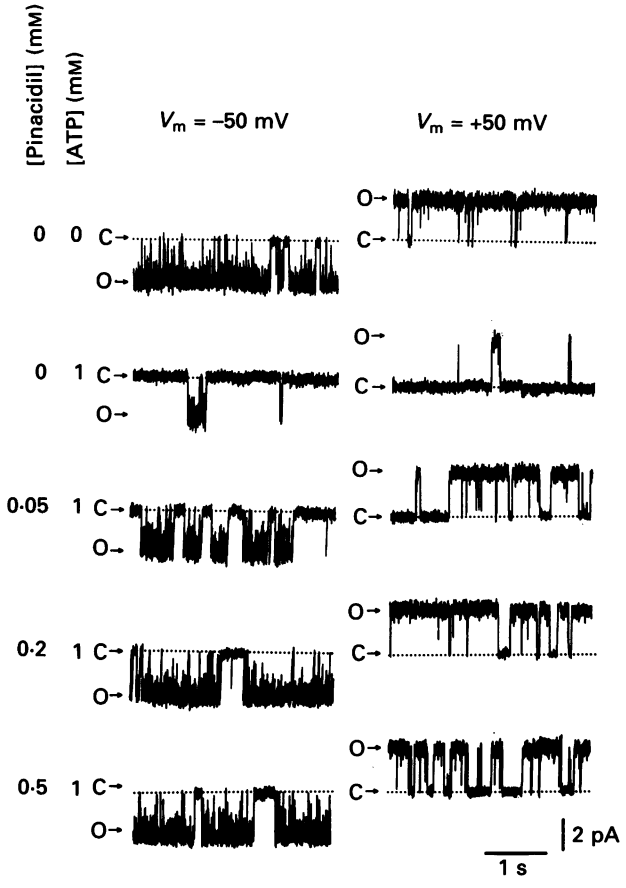

Fig. 2. Activation of the ATP-sensitive K^+ channel current by pinacidil. Records are taken from a single patch of an inside-out configuration. The concentrations of ATP and pinacidil in the bathing solution are indicated at the left side of the records. The left column shows the recordings at a membrane potential of −50 mV and the right shows those at +50 mV. The current records were filtered at f_c = 2 kHz for display.

open probability of the channel without marked changes in its unitary current amplitude. The above finding agrees with our previous observation (Fan *et al.* 1990). It was also noticed that the channel openings at +50 mV were somewhat reduced at 0·5 mM-pinacidil compared with those at 0·2 mM-pinacidil.

Figure 3*A* shows the dose–response curve of pinacidil against channel activity in the presence of 1 mM-ATP at both membrane potentials. The channel activity was expressed by normalizing P_o to that in ATP-free solution, and the activity ratio was defined as the ratio of channel activity in the presence of pinacidil to that in its absence. At the membrane potential of −50 mV, pinacidil (up to 1 mM) increased the

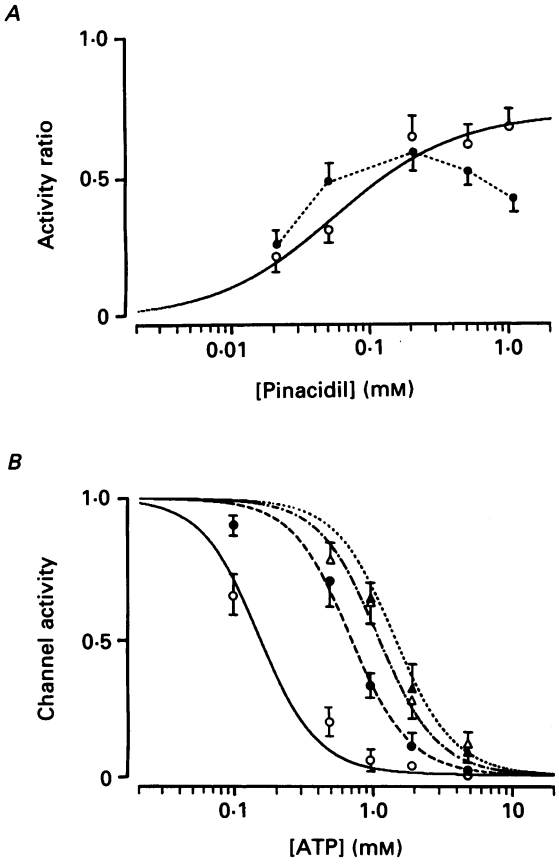

Fig. 3. Concentration–response relationship for activation of ATP-sensitive K^+ channel by pinacidil. The channel activity was expressed by normalizing the open probability (P_o) to that in ATP-free solution; and the activity ratio was defined as the ratio of channel activity with pinacidil to that without. *A*, activity ratio *vs.* [pinacidil] relationship in 1 mM-ATP solution. ○, data at $V_m = -50$ mV; ●, data at $V_m = +50$ mV. $n = 4$–7 for each point. The sigmoidal line was calculated from the model which was fitted to the data in *B*. The dotted line was used to link points at $V_m = +50$ mV. *B*, channel activity *vs.* [ATP] relationship at a pinacidil concentration of 0 (○), 0·05 (●), 0·2 (△) and 1·0 mM (▲). $n = 3$–8 for each point, pooled from total thirty-five patches. At each data point, an error bar appears whenever it is larger than the range of the symbol. Membrane potential was held at −50 mV. Lines were calculated by fitting eqn (2) to the data. See the details in the text.

channel activity in a dose-dependent manner, which could be fitted with a sigmoidal curve. The continuous line in Fig. 3*A*, as well as all the lines in Fig. 3*B*, were deduced from a theoretical fit with the model described in the next section. On the other hand, at +50 mV pinacidil was also able to increase activity up to 0·2 mM, but the activity showed a decrease thereafter, forming a bell-shaped dose–response curve.

The difference in the dose–response relationship between positive and negative potentials can be explained in several ways (see Discussion). Here we assumed a plausible mechanism: pinacidil may produce a voltage-dependent block of the

channel activity, in addition to its activation effect. For this reason, in terms of pinacidil-induced activation of the channel against ATP inhibition, it seemed appropriate to study the exact relationship between pinacidil, ATP and channel activity at a negative potential.

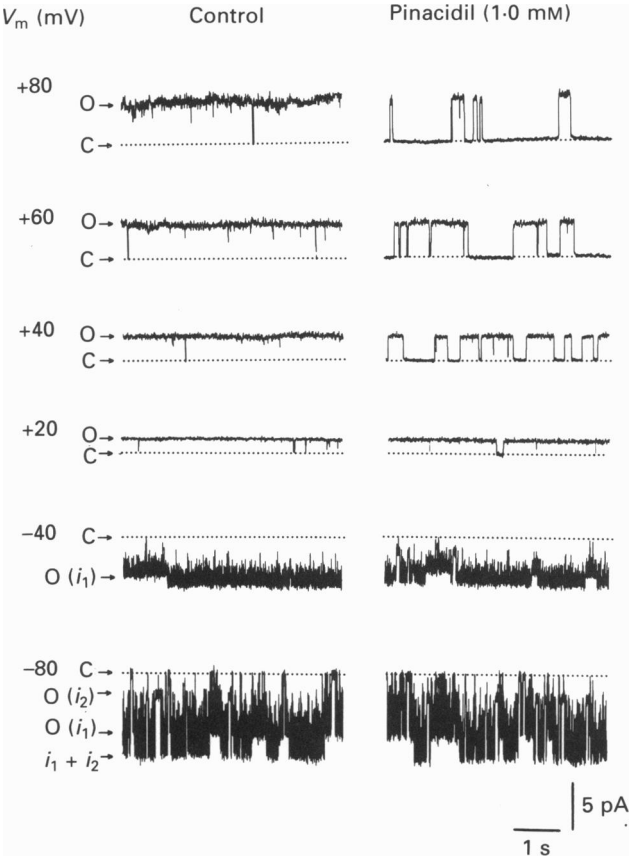

Fig. 4. Voltage-dependent block of ATP-sensitive K^+ channel currents by pinacidil in ATP-free bathing solution. The left column shows control records in the absence of pinacidil and the right those in the presence of 1 mM-pinacidil. The membrane potential is indicated on the left of the corresponding current recording. At negative potentials, the larger amplitude single-channel current (indicated by i_1) is the ATP-sensitive K^+ channel current and the smaller amplitude single-channel current (indicated by i_2) may represent the inward rectifier K^+ channel. All the records were obtained from a single patch. The current records were filtered at $f_c = 1$ kHz for display.

Figure 3*B* demonstrates the dose–response curve of the channel inhibition by ATP in the presence and absence of pinacidil at −50 mV. The data were pooled from a total of thirty-five patches. The semilogarithmic plot of the normalized channel activity against [ATP] clearly shows an antagonism between pinacidil and ATP; namely, pinacidil shifts the dose–response relationship of ATP inhibition to the right without changing the slope of the relationship. The plot also illustrates that the

maximal effect of pinacidil to activate the channel is depressed and the half-saturation pinacidil concentration is increased with an increase in ATP concentration. Consequently, the shift in the dose–response curve of ATP inhibition appeared to approach a limiting value as pinacidil concentration was increased higher than 0·2 mM. This implies that the antagonism is not competitive. A model is now proposed to explain the antagonism between pinacidil and ATP.

Model for the antagonism between pinacidil and ATP

Since we do not know the details of the reaction, the model can only give an overall description of the relationship between [pinacidil], [ATP] and channel activation, rather than a strict kinetic mechanism. The model is based on the assumption that the binding of ATP and pinacidil to the sites in the patch membrane follows the basic principles of receptor theory. It is also assumed that the inhibition of P_o can be considered proportional to the probability that the receptor is occupied by ATP. According to receptor theory (Boeynaems & Dumont, 1980), our observation that pinacidil shifted the dose–response relationship of ATP inhibition to the right without a change in slope and that the shift approached a limiting value at increased pinacidil concentration can be explained by pseudo-competitive antagonism. Pursuing the theory, we postulate that pinacidil and ATP are bound to the same receptor but at different sites; therefore the receptor can form either ATP–receptor or pinacidil–ATP–receptor complexes, and either complex has the same efficacy in relation to channel activity. Previous reports (Kakei *et al.* 1985; Lederer & Nichols, 1989; Ribalet, Ciani & Eddlestone, 1989), as well as our data presented in Fig. 3*B*, indicate that the dose–response relationship for ATP inhibition can be expressed by a Hill function with a Hill coefficient higher than 1. This suggests a model in which two ATP molecules are necessary to form the complex with the receptor. Thus, a cyclic scheme can predict the antagonism between pinacidil and ATP:

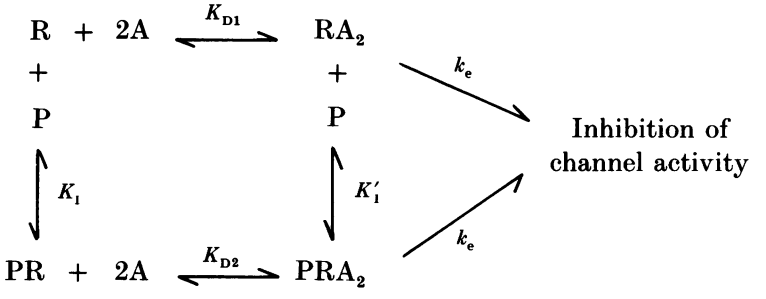

(S1)

where R, P and A stand for the unoccupied receptor, pinacidil and ATP, respectively. K_{D1}, K_{D2}, K_I and K'_I are the overall equilibrium dissociation constants for the four steps of the cyclic reaction, and k_e is the proportionality factor linking the occupation of the receptor and channel activity. In this scheme, the receptor complexes formed by the occupation of one ATP molecule are neglected for simplification. According to this scheme, the channel activity can be related to pinacidil concentration ([P]) and ATP concentration [A] by:

$$\text{channel activity} = 1-([A]^2/([A]^2+K_{D1}(K_I+[P])/(K_I+K_{D1}[P]/K_{D2}))). \quad (2)$$

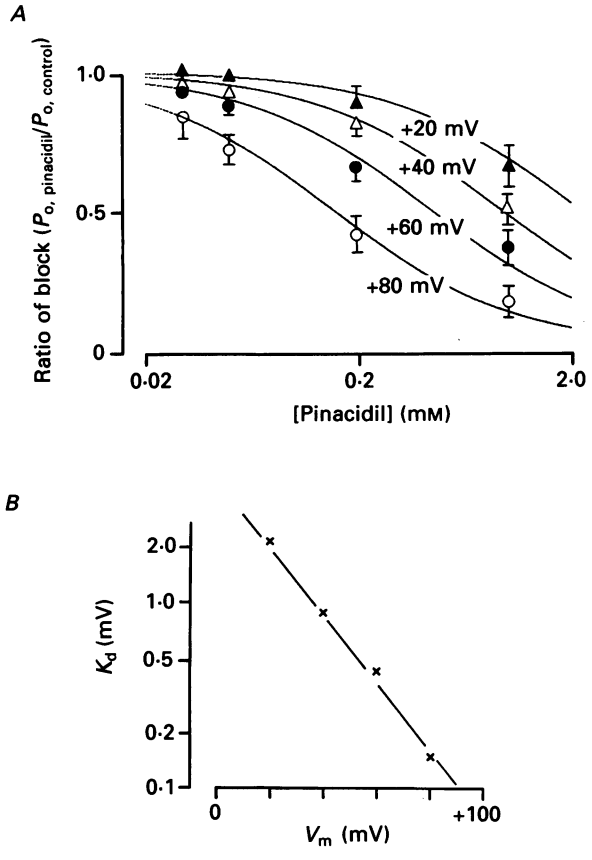

Fig. 5. Voltage-dependent block of ATP-sensitive K^+ channels by pinacidil. A, voltage- and concentration–response relationships for pinacidil block. Abscissa, logarithmic [pinacidil] (in mM); ordinate, extent of block expressed as the ratio of P_o with pinacidil to that without. Extent of block was obtained at various pinacidil concentrations and four different membrane potentials. Different symbols (▲, △, ●, ○) correspond to different voltages (+20, +40, +60, +80 mV, respectively). $n = 3$–6 for each point, from a total of seven patches. At each data point, an error bar appears whenever it is larger than the range of the symbol. The continuous lines are the fits of eqn (4) to the data with values for K_d of 2·2, 0·92, 0·43 and 0·15 mM, respectively. *B*, voltage dependence of the dissociation constant, K_d, for pinacidil block. Values of K_d were calculated from the ratio of block shown in *A*. The line is drawn corresponding to eqn (5) in the text, with $K_d(0) = 5{\cdot}2$ mM and $z' = 1{\cdot}09$.

Our experimental results are compatible with such a relation, because the data points in Fig. 3 can be well fitted to eqn (2) (as shown by the lines). The equilibrium dissociation constants determined by fitting were: $K_{D1} = 2{\cdot}25 \times 10^{-2}$ mM^2; $K_{D2} = 2{\cdot}56$ mM^2; $K_I = 2 \times 10^{-3}$ mM; and $K'_I = 0{\cdot}228$ mM (where K'_I is determined by microscopic reversibility). The half-saturation pinacidil concentration (denoted by $[P]_{0{\cdot}5}$) to activate the channel under an ATP concentration is given by

$$[P]_{0{\cdot}5} = K_I(1+[ATP]^2/K_{D1})/(1+[ATP]^2/K_{D2}). \quad (3)$$

For example, in Fig. 3*A* where [ATP] = 1 mM, $[P]_{0.5}$ = 0·07 mM.

Block of ATP-sensitive K^+ current by pinacidil

Voltage- and concentration-dependent block

As stated in the first section, we hypothesize that pinacidil may also induce block of channel activity. Since pinacidil antagonizes ATP to modulate channel gating, its blocking action was examined under ATP-free conditions where the channel open probability was high (Fig. 4). At positive voltages, the channel opening was interrupted by long closures showing burst behaviour only in the presence of 1 mM-pinacidil, while the unitary amplitude of the single-channel current was unchanged. At negative voltages, however, no changes in the behaviour of channel opening were noted after application of pinacidil. Therefore, pinacidil produced a voltage-dependent block of the channel. In this patch, another channel of smaller unitary amplitude was present, but we did not analyse its behaviour in this study since it was not blocked by ATP.

Under ATP-free conditions, the pinacidil-induced block was studied quantitatively in seven patches, expressed as the ratio of P_o in the presence of the drug to that in its absence. The results obtained at different pinacidil concentrations and various positive potentials are summarized in Fig. 5*A*. The block became stronger at the higher voltage with increasing pinacidil concentration. The data from the same potential but different concentrations were well fitted to a first-order Hill saturation function:

$$\text{ratio of block} = 1/\{1+([\text{pinacidil}]/K_d)\}, \tag{4}$$

where K_d (the dissociation constant) was 2·2, 0·92, 0·43 and 0·15 mM for +20, +40, +60 and +80 mV, respectively. Meanwhile, we were unable to detect any block at negative potentials.

The relationship between voltage and K_d can be fitted by an exponential function:

$$K_d = K_d(0)\exp(-z'V_mF/RT), \tag{5}$$

where $K_d(0)$ = 5·2 mM is the expected value of K_d at V_m = 0 mV and equivalent valency z' = 1·09 which represents the sensitivity of K_d to the electric field with an e-fold change per 23 mV (Fig. 5*B*).

Blocking kinetics

While either one open state and two closed states, or two open and closed states, are generally considered to account for the gating kinetics of the ATP-sensitive K^+ channel (Kakei *et al.* 1985; Spruce *et al.* 1987; Ashcroft, 1988), our previous analyses of the distributions of open and closed times indicated the following kinetic scheme (Fan *et al.* 1990):

$$C_3 \underset{k_{-3}}{\overset{k_3}{\rightleftharpoons}} C_2 \underset{k_{-2}}{\overset{k_2}{\rightleftharpoons}} O \underset{k_{-1}}{\overset{k_1}{\rightleftharpoons}} C_1, \tag{S2}$$

where the transition between O and C_1 was thought to depend on the carrier flux through the channel (Zilberter, Bernashev, Papin, Portnov & Khodorov, 1988),

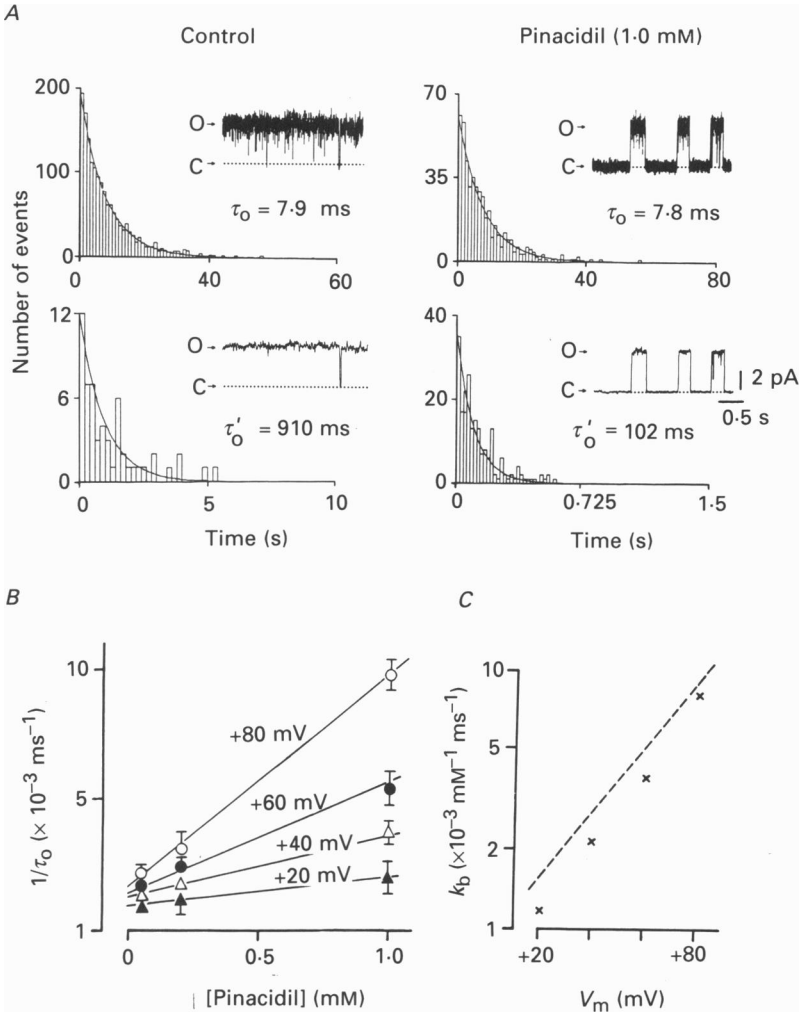

Fig. 6. Effect of pinacidil on open-time distribution. *A*, the left column shows the open-time histograms under control conditions and the right column shows those in the presence of pinacidil. In the upper panels, open-time distributions were analysed with f_c = 7·5 kHz. In the lower panels, open-time distributions were analysed with f_c = 0·1 kHz. The insets are examples of corresponding current records. The continuous lines are drawn by a single exponential. V_m = +80 mV. *B*, plot of the reciprocal of the mean open time at f_c = 0·1 kHz against pinacidil concentration. Different symbols (▲, △, ●, ○) correspond to different membrane potentials (+20, +40, +60, +80 mV, respectively). n = 4–7 for each point. At each data point, an error bar appears whenever it is larger than the range of the symbol. The continuous lines are drawn by a linear function with a slope representing the blocking rate constant k_b, and the values are 1·2, 2·2, 3·8 and 8·0 × 10^{-3} mM^{-1} ms^{-1}, respectively. *C*, voltage dependence of k_b. The points are obtained from *B*. The dashed line is drawn from k_{-b}/K_d, and corresponds to eqn (5) in the text giving $k_b(0)$ = 9·3 × 10^{-4} mM^{-1} ms^{-1} and z' = 0·7.

while the transitions between O, C_2 and C_3 were ligand-regulated processes. Since the pinacidil-induced block was studied in the absence of ATP, it was possible to rearrange the kinetic model in a simpler form, assuming that the blocking process by pinacidil obeys a first-order reaction:

$$\begin{array}{ccc} & \overset{k_1}{} & \\ O & \rightleftharpoons & C_1 \\ & \underset{k_{-1}}{\uparrow} & \\ k_b[\text{pinacidil}] & \downarrow & k_{-b} \\ & B & \end{array} \qquad \text{(S3)}$$

where k_b and k_{-b} are the rate constants for blocking and unblocking, so that the dissociation constant $K_d = k_{-b}/k_b$.

An analysis of the open-time distribution is given in Fig. 6*A*. The membrane potential was held at +80 mV. When the records were filtered with $f_c = 7{\cdot}5$ kHz, the open-time histogram was best expressed by a single-exponential distribution with a time constant of 7·9 ms, which was not changed (7·8 ms) by application of 1·0 mM-pinacidil. However, when the same record was analysed after passing through a 100 Hz filter, the detectable mean open time in the control was prolonged to 910 ms since most of the short closures were omitted by the filter. With this low filter frequency, pinacidil markedly shortened the distribution of the open time to 102 ms. Since the mean duration of brief closures of the ATP-sensitive K^+ channel becomes shorter near the reversal potential at positive voltages (Zilberter *et al.* 1988), the records filtered at $f_c = 100$ Hz seem suitable for analysis of the pinacidil effect on open time. The data from eight patches at different pinacidil concentrations are summarized in Fig. 6*B*. The mean open time showed both voltage and concentration dependence, becoming shorter at higher positive potentials and with increasing pinacidil concentration. In Fig. 6*B*, the ordinate represents the reciprocal of the mean open time, which should be a linear function of pinacidil concentration and, therefore, according to the scheme (S3) the reciprocal of the mean open time is proportional to pinacidil concentration with a slope of k_b.

The points at three pinacidil concentrations could be well fitted by straight lines ($r_s > 0{\cdot}98$). The slope of the line gave an estimate of the blocking rate constant. (We say 'estimate' because the 100 Hz filter used to isolate pinacidil-induced burst behaviour from the intrinsic openings of the channel may cause distortion in the concentration relationship. The intercept of the line in Fig. 6*B*, which should equal the reciprocal of the mean open time with the 100 Hz filter, differs from that measured at higher frequencies.) The values of k_b decreased at less positive potentials, from $8{\cdot}0 \times 10^{-3}$ mM^{-1} ms^{-1} at +80 mV to $1{\cdot}2 \times 10^{-3}$ mM^{-1} ms^{-1} at +20 mV (Fig. 6*C*). The dashed line in the figure is the predicted value of k_b calculated from K_d and k_{-b}. (Measurement of k_{-b} will be described later.) The line also gives $k_b(0) = 9{\cdot}3 \times 10^{-4}$ mM^{-1} ms^{-1} and equivalent valency $z' = 0{\cdot}7$, derived from eqn (5) by substituting $K_d(0)$ with $k_b(0)$ and the minus sign with a plus. The small deviations of measured values from predicted ones may be caused by the analyses with a 100 Hz filter.

Closed times were analysed with $f_c = 7{\cdot}5$ kHz. In Fig. 7*A* an example of this analysis is given. In ATP-free solution at +80 mV, when the bin width was set at

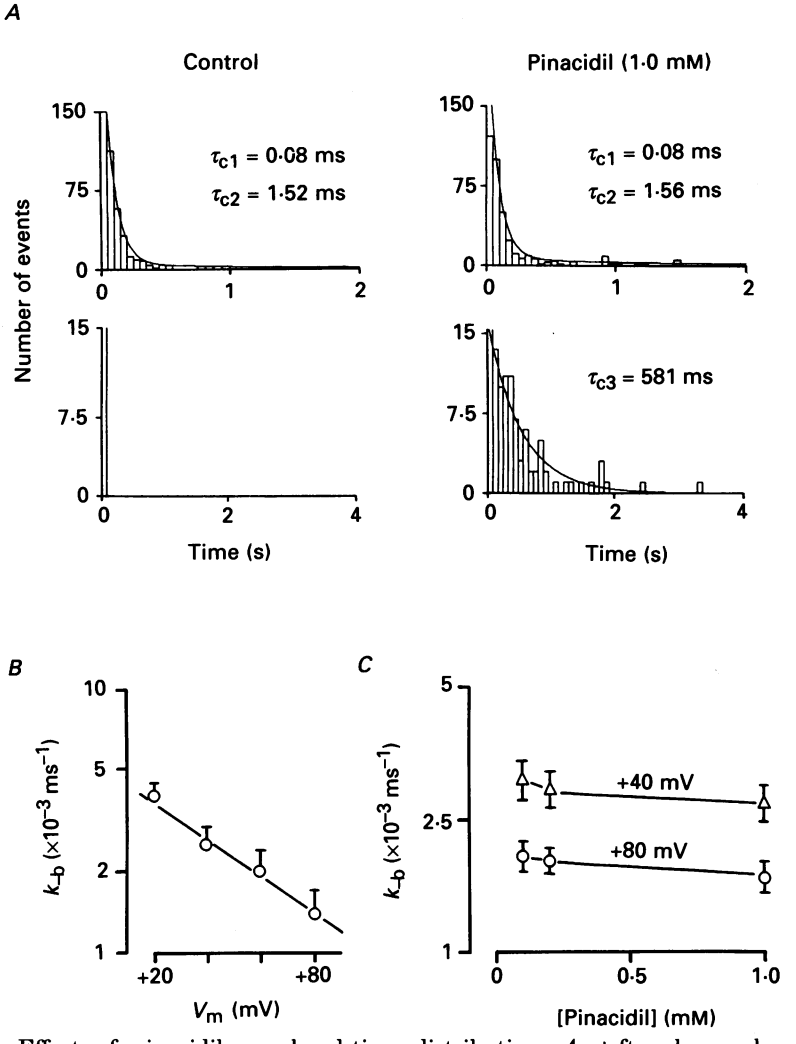

Fig. 7. Effect of pinacidil on closed-time distribution. *A*, left column shows the histograms of closed time under control conditions and the right column shows those in the presence of pinacidil. In the upper panels, closed-time distributions were analysed with bin width = 5 ms and in the lower panels, closed-time distributions were analysed with bin width = 40 ms. The continuous lines are drawn by two exponentials in the upper panels, and by a single exponential in the right lower panel. $V_m = +80$ mV. *B*, voltage dependence of the unblocking rate constant, k_{-b}, calculated from the reciprocal of the closed time constants at bin width = 40 ms. The values of k_{-b} are 3·72, 2·75, 2·0 and $1{\cdot}45 \times 10^{-3}$ ms^{-1} at +20, +40, +60 and +80 mV, respectively. $n = 4$–5 for each point from a total of five patches. The line is drawn from the data corresponding to eqn (5), with $k_{-b}(0) = 5{\cdot}1 \times 10^{-3}$ ms^{-1} and $z' = 0{\cdot}39$. *C*, plot of k_{-b} against [pinacidil] at +40 mV (○) and +80 mV (△). $n = 3$–5 for each point. All the closed-time distributions were analysed with $f_c = 7{\cdot}5$ kHz.

0·05 ms, the mean closed time could be fitted to a two-exponential function with $\tau_{c1} = 0{\cdot}08$ ms and $\tau_{c2} = 1{\cdot}52$ ms. The amplitude of the slow component was negligible. Application of 1 mM-pinacidil did not produce changes in either of these components, but a much slower component emerged that was not present in the control. When analysed with a bin width of 40 ms this component showed a single-exponential distribution. The time constant was voltage dependent and increased with membrane depolarization. Since this time constant did not overlap with those in the control, its reciprocal can be taken as a direct measurement of the unblocking rate, k_{-b}. The values of k_{-b} from five patches are plotted in Fig. 7*B* and they decrease as the voltage increases. k_{-b} can be fitted to eqn (5) with parameters of $k_{-b}(0) = 5{\cdot}1 \times 10^{-3}$ ms^{-1} and $z' = 0{\cdot}39$. For scheme (S3) and this calculation, it was assumed that k_{-b} did not depend on pinacidil concentration. The measured data from nine patches at three pinacidil concentrations are summarized in Fig. 7*C* to confirm this point.

Time-dependent development of block

The above kinetic analysis demonstrated that the pinacidil-induced block was well fitted to a slow first-order transition process with a time range of 10^2–10^3 ms. Moreover, the block showed a voltage dependence, with complete relief at negative potentials. Therefore, it can be supposed to record a time-dependent development of the block and unblock when the voltage is stepped between negative and positive values. In ten patches, a stepped voltage protocol, from −70 mV to different positive voltages having a duration of 2·7 s, was applied every 6 s (Fig. 8*A*). In the presence of 0·2 mM-pinacidil, no block occurred initially after the voltage was stepped from −70 mV to +50 mV, but block developed with time, gradually reaching a steady state. This process is illustrated clearly and quantitatively in ensemble current when the single-channel current is averaged, showing an exponential decay with time in the ensemble current. The time constant of the decay was voltage dependent. The relationship between the time constant and the voltage had a concave shape with a maximum at around +50 mV (Fig. 8*B*). The time constant was also predicted from the blocking and unblocking rate constants, k_b and k_{-b}, using the equation:

$$\text{time constant} = 1/(k_b[\text{pinacidil}] + k_{-b}]. \quad (6)$$

The calculated time constants were in general agreement with those measured for steps in the voltage range from +20 to +80 mV (dashed line in Fig. 8*B*).

In contrast to the slow time-dependent development of the block, the unblocking process upon return to −70 mV was almost instantaneous, showing no time-dependent changes in the single-channel or averaged current records (Fig. 8*A*). This was because the time constants became very short at negative voltages (Fig. 8*B*).

Restoration of the channel activity by pinacidil after 'run-down'

In the inside-out patch configuration, the activity of the ATP-sensitive K^+ channel gradually decreased with time due to run-down (Fig. 9*A*, early phase). In ATP-free solution with a Ca^{2+} concentration of less than 10^{-9} M, the P_o of the channels in about 80% of patches decreased to less than 0·001 within 12–20 min (six out of eight patches from four animals). This spontaneous run-down was strongly enhanced by

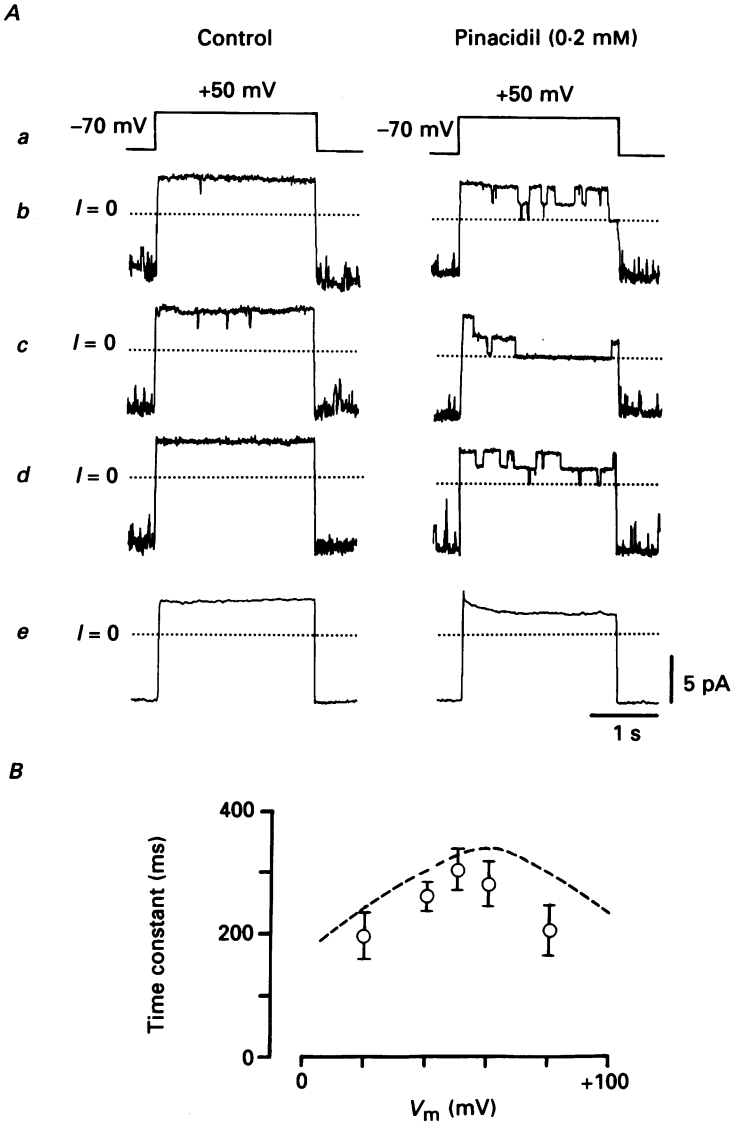

Fig. 8. Pinacidil-induced decay of single-channel current. *A*: *a*, voltage protocol, *b–d*, current records before or after the application of pinacidil; *e*, averaged currents of forty (control) or thirty (pinacidil) current records. The decay of the averaged current in the presence of pinacidil can be fitted to a single exponential. Capacitative and leakage currents are subtracted from the records. Current records were filtered at f_c = 0·1 kHz. *B*, voltage dependence of time constants of averaged current decay induced by 0·2 mM-pinacidil. n = 4–6 for each point. The dashed line is calculated from k_b and k_{-b} by eqn (6).

a short exposure of the internal surface of the membrane to a solution containing 1 mM-Ca^{2+} (Fig. 10*A*, early phase). The channel activity was usually suppressed, and stopped within 15–30 s after exposure to the Ca^{2+}-containing solution (total of fifteen patches). For both spontaneous and Ca^{2+}-induced run-down, application of 0·1 mM-

pinacidil partially reactivated the channel (Figs 9*A* and 10*A*, later phases). Removal of pinacidil caused the channel activity to return to a low level. Similar effects were also observed in 0·03 mM-pinacidil, but the response was less marked than those in 0·1 mM-pinacidil solution ($n = 5$). In Fig. 9*B*, channel flickerings are similar before

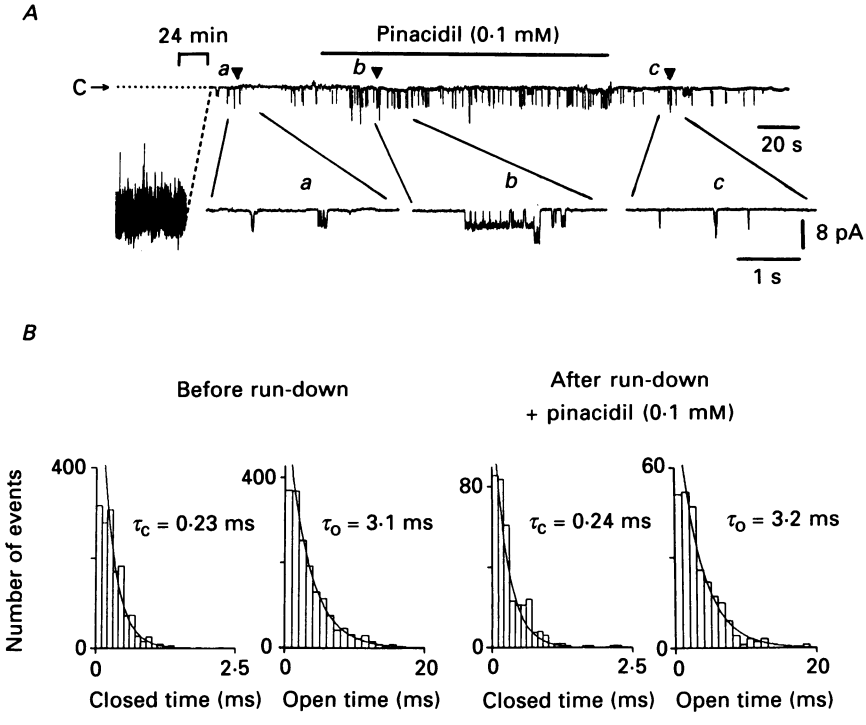

Fig. 9. *A*, restoration of the channel activity by pinacidil after spontaneous run-down of the channel activity. Recording from a cell-free patch containing eight channels. The continuous recordings are interrupted by 24 min. Expansions of the records at the times marked by ▼ are shown in the lower panels under each record. Membrane potential was held at −50 mV. *B*, histograms of open and closed times before the channel run-down in the absence of pinacidil, and after the channel run-down in the presence of 0·1 mM-pinacidil. The data are from two separate patches. $f_c = 5$ kHz. $V_m = -50$ mV. The histograms are fitted by a single exponential.

run-down and after restoration of the channel activity by pinacidil. No changes in either the open- or closed-time distribution were noted.

The degree of restoration of the channel activity by pinacidil depended on the conditions of the patch and the time course of the run-down. Figure 10*B* shows an example of the record using an open-cell patch configuration. The cell membrane was chemically permeated by 0·05 mM-digitonin (Kakei *et al.* 1985). The channels opened after penetration of the membrane and were then shut by application of 1 mM-Ca^{2+} for 1 min. Application of 0·1 mM-pinacidil reactivated the channel to a much greater degree than in the case of the cell-free patches shown in Fig. 10*A*. In Fig. 10*C*, it can be seen that the restoration was also influenced by the time course of the run-down. When pinacidil was applied to the cell-free membrane within 1 min after Ca^{2+}

treatment, the pinacidil-induced restoration was apparently stronger than that shown in Fig. 10*A* where pinacidil was applied 3 min after Ca^{2+} treatment. Figure 11 summarizes the results from a total of sixteen patches. The difference in P_o between cell-free and open-cell patches is significant. Reactivation by pinacidil after the

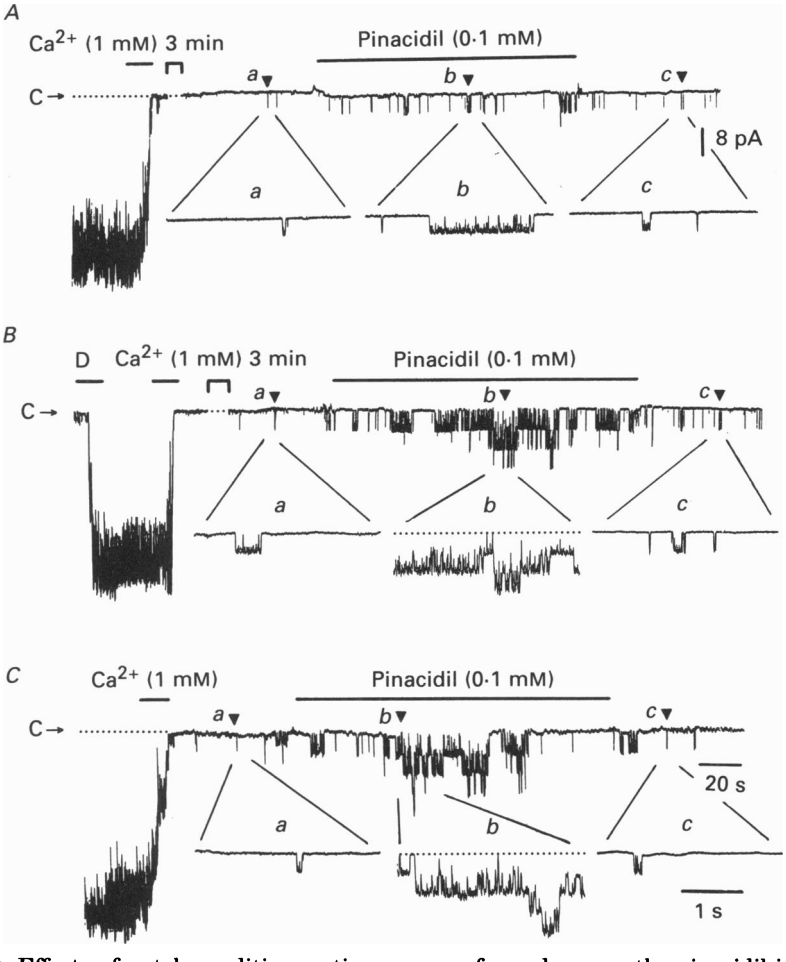

Fig. 10. Effects of patch condition or time course of run-down on the pinacidil-induced restoration of channel activity. *A*, pinacidil-induced reactivation in a cell-free patch membrane. The run-down of the channels was caused by application of 1 mM-Ca^{2+} for 1 min. Pinacidil (0·1 mM) was applied to the patch 3 min after a wash-out of Ca^{2+}-containing solution. *B*, pinacidil-induced reactivation in an open-cell patch. The cell was permeated with 0·05 mM-digitonin (D) at the time indicated. *C*, pinacidil-induced reactivation in a cell-free patch. Pinacidil was applied to the patch 45–60 s after suppression of the channel activity by 1 mM-Ca^{2+}. In *A*, *B* and *C*, $V_m = -50$ mV.

shorter period of inactivation ($T < 1$ min) is also significantly stronger than that after the longer period ($T > 3$ min).

The above results imply that the reactivation by pinacidil may possibly depend upon certain intracellular factors. The experiment shown in Fig. 12 supports this

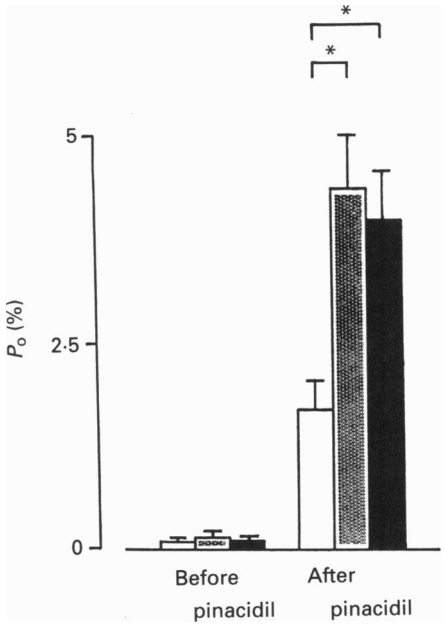

Fig. 11. Effects of pinacidil on channel activity after run-down. P_o was calculated using a 1 min length of record in the absence of pinacidil and a 1 min length of record in the presence of 0·1 mM-pinacidil where the maximal response appeared. T is the interval between the withdrawal of 1 mM-Ca^{2+} from the solution and the time when pinacidil was added to the bath. $n = 7, 4, 5$ for $T > 3$ min and cell-free mode (□), $T > 3$ min and open-cell mode (▨), $T < 1$ min and cell-free mode (■), respectively. Data are from sixteen separate patches. $*P < 0.05$.

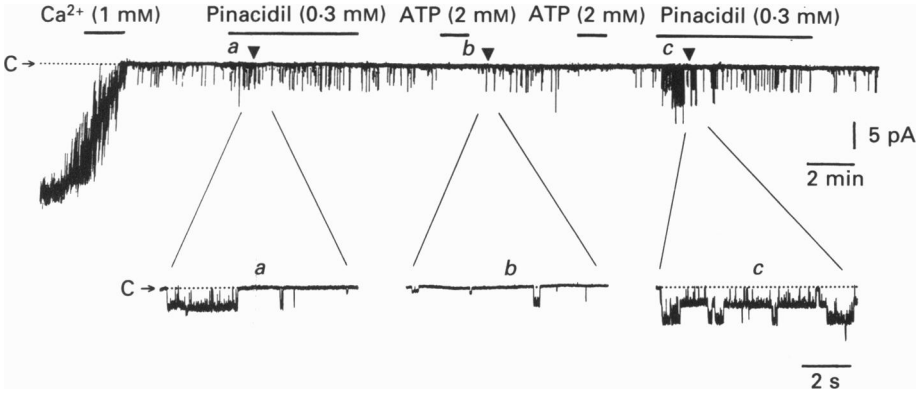

Fig. 12. Effect of pre-treatment of ATP on the pinacidil-induced reactivation. $V_m = -50$ mV. Expansions of the records at the times marked by ▼ are shown in the lower panels. For further explanation, see text.

possibility. In this experiment, the run-down was induced by applying Ca^{2+} and pinacidil (0·3 mM) was then applied to the inside-out patch membrane 3 min later. The activity of the channel was increased to a minor extent. After wash-out of the pinacidil, application of 2 mM-ATP for 1 min stopped the residual channel activity.

Removing ATP from the bathing solution restored the channel activity to a level not different from that before application of ATP. The membrane was then re-exposed to ATP. After complete removal of ATP from the bathing solution, 0·3 mM-pinacidil was then applied to the membrane. The activity enhanced by pinacidil after pre-treatment with ATP was much larger than that by the first application of pinacidil where the membrane was not pre-treated with ATP. This result was confirmed in six patches. Note that the concentrations of free Mg^{2+} in both ATP-free and 2 mM-ATP solutions were 5×10^{-6} M or less (see Methods).

DISCUSSION

Different binding sites

It is generally accepted that a special binding site is located on the intracellular side of the membrane by which ATP closes the ATP-sensitive K^+ channel (Ashcroft, 1988). The characteristics of this binding site include: (1) accessibility to various nucleotides such as other adenine nucleotides, pyrimidine nucleotides and purine nucleotides, with maximum affinity for ATP, (2) lack of association with pre-phosphorylation, and (3) lack of sensitivity to the membrane potential. Our present data showed that pinacidil shifts the dose–response curve for ATP to the right, and, at the same time, inhibits channel opening. Pre-phosphorylation of the channel does not seem to be necessary for these two effects of pinacidil since Mg^{2+} is extremely low. Furthermore, the inhibition can occur in the absence of ATP. It might therefore be suggested that pinacidil is a partial agonist with a highly competitive binding affinity for the ATP site, so that the observed inhibition is due to the intrinsic activity of pinacidil. A similar mechanism was proposed for the dual action of ADP on channel activity (Dunne & Petersen, 1986; Kakei, Kelly, Ashcroft & Ashcroft, 1986; Dunne, West-Jordan, Abraham, Edwards & Petersen, 1988; Findlay, 1988). However, this explanation was ruled out by the remarkably different voltage sensitivities for activation and block of the channel by pinacidil. Therefore, we favour the hypothesis of multiple binding sites: one for activation and another for block. A family of first-order dose–response curves was well fitted to the pinacidil-induced block at different voltages, which also indicates a specific type of binding for block. However, the present results do not provide sufficient evidence to support the existence of different sites for pinacidil-induced activation of the channel before its run-down and subsequent reactivation.

Mechanism of channel activation by pinacidil

Since the ATP-sensitive K^+ channel opens in the absence of ATP, it is difficult to discriminate directly a true 'opener' of the channel from an antagonist of the ATP binding process. However, we have found previously in kinetic analysis of channel gating that pinacidil induces a change similar to that of reduced ATP concentration (Fan *et al.* 1990). Our present experiments further showed that the activation effect of pinacidil depended on the ATP concentration. Therefore, it is plausible that pinacidil cannot directly open the channel. The same suggestion was also made by other researchers (Arena & Kass, 1989).

The fact that pinacidil shifts the dose–response relationship of ATP inhibition to

the right suggests that pinacidil opens the channel by antagonizing ATP binding. However, pinacidil is not a pure competitive antagonist since the inhibition by increasing ATP concentration cannot be fully antagonized by increasing pinacidil concentration. Also, as discussed in the last section, no evidence exists to propose pinacidil as a partial agonist. Therefore, it can be assumed that pinacidil does not compete with ATP at its binding site(s).

We therefore speculated that pinacidil binds to a different site and modulates the affinity of the receptor to ATP, i.e. the antagonism is a pseudo-competitive process. That the model (S1) was well fitted to the experimental data supported the above idea. The model predicts that: (1) ATP inhibits the channel activity with a half-saturation concentration of $\sqrt{K_{D1}}$, which was 0·15 mM from fitting, a value close to that of other reports (Ashcroft, 1988; Qin, Takano & Noma, 1989); (2) pinacidil shifts the point to the right with a maximum at $\sqrt{K_{D2}}$; (3) $[P]_{0.5}$ varies with ATP concentration, between a minimum at K_I when the ATP concentration is approaching zero, and a maximum at $K_I(K_{D2}/K_{D1})$, i.e. K'_I, at an infinitely high ATP concentration; (4) the maximal effect of pinacidil decreases towards zero with the increase of ATP concentration. All of these features have been found experimentally, not only in the single-channel recording presented in this paper, but also in the whole-cell recording (unpublished observations).

Kinetic properties of the block

The dose–response curve at a given membrane potential for the block of the ATP-sensitive K^+ channel by pinacidil can be well fitted to a first-order saturation function, showing specific one-to-one binding. The dissociation constant K_d sharply varies with voltage. The channel-gating kinetics produced by pinacidil follows a first-order transition (S3) process. All the results are consistent with the model that pinacidil binds to a specific site in the pore of the channel pathway, producing physical plugging. A similar model was used to explain many other voltage-dependent blockers (Hille, 1984). According to such a model and the Eyring rate theory, we found three important features of the block: first, $k_b(0)$ and $k_{-b}(0)$ are inversely proportional to the magnitude of the energy barrier against the entry and exit of pinacidil through the inner mouth of the channel. These parameters were estimate to be $1{\cdot}1 \times 10^3$ ms mM and $2{\cdot}0 \times 10^2$ ms, respectively. These values indicate that it is difficult for pinacidil to jump into the site without the aid of electromotive force. Second, the equivalent valency, or the voltage sensitivity factor, z', is the product of a partition parameter (denoted as d) and the valency of the charged form of the pinacidil molecule. Supposing that 90% of the charged form of pinacidil in the perfusate at pH 7·3 is in the form of monovalent ions while the rest is divalently charged, then the value of d for k_b could be estimated as 0·6 and that for k_{-b} as 0·3. They represent the fractional electrical distance from the inner mouth of the channel to the peak of the energy barrier, and the distance from the peak to the binding site, respectively. Their sum, 0·9, represents the depth of the binding site in the membrane from the inner mouth of the channel. These data are in agreement with the assumption of a single-file energy barrier. Third, the values of $k_b = 8{\cdot}0 \times 10^{-3}$ mM^{-1} ms^{-1} and $k_{-b} = 1{\cdot}45 \times 10^{-3}$ ms^{-1} at +80 mV indicate a very slow binding process, which has not been found among all the other well-studied blockers for this channel.

TEA has been found to produce a slow block from the inner side of the membrane on the ATP-sensitive K^+ channel in frog skeletal muscle, with $k_b = 0{\cdot}3$ mM^{-1} ms^{-1} and $k_{-b} = 0{\cdot}2$ ms^{-1} (Davies, Spruce, Standen & Stanfield, 1989). A similar type of blocking by TEA was also seen in cardiac cells (Kakei *et al.* 1985). Both TEA and pinacidil have a large molecular diameter. Therefore, the fact that they produce voltage-dependent block from the inner side of the membrane suggests that the outer mouth of the ATP-sensitive K^+ channel is narrower than the inner mouth. Yet ions of smaller diameter, such as Ba^{2+}, can block the channel from the outside of the membrane, with $k_b = 2$ mM^{-1} ms^{-1} and $k_{-b} = 0{\cdot}08$ ms^{-1} at -80 mV (Quayle, Standen & Stanfield, 1988). Mg^{2+}, Na^+ and Cs^+ can block the channel from either the inner or outer side of the membrane. Their binding kinetics are much faster than those of pinacidil (Horie, Irisawa & Noma, 1987; Quayle *et al.* 1988).

Reactivation of the run-down channel by pinacidil

After run-down of the ATP-sensitive K^+ channel, application of Mg^{2+}-ATP could restore the channel activity, whereas Na^+-ATP and ATP analogues such as AMP-PMP were not effective in restoring activity (Findlay, 1987*a*, *b*). Run-down has therefore been suggested to be associated with a loss of channel phosphorylation (Ashcroft, 1988; Takano, Qin & Noma, 1990). However, the run-down seems not to be a simple process. The channel may undergo several conformation changes during run-down. Findlay (1988) showed that ADP in the presence of Mg^{2+} was able to activate the channel after pre-treatment with Mg^{2+}-ATP. In the present work, it was not only shown that the run-down channel could be partially reactivated by pinacidil, but also that the reactivation effect depended on the conditions of the patch membrane. The ability of pinacidil to reactivate the channel was also diminished with time. We further observed that pre-treatment of the channel with ATP after run-down considerably strengthened the reaction effect of pinacidil, while ATP with low Mg^{2+} could not restore the channel activity, which is similar to findings obtained by others (Trube & Hescheler, 1984; Ashcroft, 1988). Although this study was not designed to investigate the detailed mechanism of the run-down process, our findings demonstrate that even after the channel failed to open due to run-down the ability of the channel to be reactivated was still changing and such change also depended on some intracellular factors. A reactivation effect was also reported for cromakalim, an agent which can open ATP-sensitive K^+ channels (Escande *et al.* 1989). Reactivation by these agents offers information which cannot be observed directly from the behaviour of channel openings and closings. Further clarification of the reactivation mechanism may be helpful for understanding the run-down process of the channel.

Conclusion

We demonstrated that the ATP-sensitive K^+ channel in guinea-pig ventricular cells is modulated by pinacidil. Pinacidil caused either activation, block or reactivation of channel opening. Such multiple actions suggest multiple binding sites for pinacidil. The relationship between [pinacidil], [ATP] and channel activity provides evidence on the pattern of the antagonism between pinacidil and ATP, and thus is important for further clarifying the mechanism of the pharmacological effect

of this agent. The data about the block and reactivation, on the other hand, have more physiological importance. Use of pinacidil as a pharmacological tool could extend our knowledge of the physiology of the ATP-sensitive K^+ channel.

The authors wish to thank Dr Jonathan C. Makielski, the University of Chicago, for reading the manuscript.

REFERENCES

ARENA, J. P. & KASS, R. S. (1989). Enhancement of potassium-sensitive current in heart cells by pinacidil: evidence for modulation of the ATP-sensitive potassium channel. *Circulation Research* **65**, 436–445.

ASHCROFT, F. M. (1988). Adenosine 5′-triphosphate-sensitive potassium channels. *Annual Review of Neuroscience* **11**, 97–118.

BOEYNAEMS, J. M. & DUMONT, J. E. (1980). *Outlines of Receptor Theory*. North Holland Biomedical Press/Elsevier, Amsterdam.

COOK, D. L. & HALES, C. N. (1984). Intracellular ATP directly blocks K^+ channels in pancreatic B-cells. *Nature* **311**, 271–273.

DAVIES, N. W., SPRUCE, A. E., STANDEN, N. B. & STANFIELD, P. R. (1989). Mulitple blocking mechanisms of ATP-sensitive potassium channels of frog skeletal muscle by tetraethylammonium ions. *Journal of Physiology* **413**, 31–48.

DUNNE, M. J. & PETERSEN, O. H. (1986). Intracellular ADP activates K^+ channels that are inhibited by ATP in an insulin-secreting cell line. *FEBS Letters* **208**, 59–62.

DUNNE, M. J., WEST-JORDAN, J. A., ABRAHAM, R. J., EDWARDS, R. H. T. & PETERSEN, O. H. (1988). The gating of nucleotide-sensitive K^+ channels in insulin-secreting cells can be modulated by changes in the ratio ATP^{4-}/ADP^{3-} and by nonhydrolyzable derivatives of both ATP and ADP. *Journal of Membrane Biology* **104**, 165–177.

ESCANDE, D., THURINGER, D., LEGUERN, S., COURTEIX, J., LAVILLE, M. & CAVERO, I. (1989). Potassium channel openers act through an activation of the ATP-sensitive K^+ channels in guinea-pig cardiac myocytes. *Pflügers Archiv* **414**, 669–675.

FABIATO, A. & FABIATO, F. (1979). Calculator programs for computing the composition of the solutions containing multiple metals and ligands used for experiments in skinned muscle cells. *Journal de physiologie* **75**, 463–505.

FAN, Z., NAKAYAMA, K. & HIRAOKA, M. (1990). Pinacidil activates the ATP-sensitive K^+ channel in inside-out and cell-attached patch membranes of guinea-pig ventricular myocytes. *Pflügers Archiv* **415**, 387–394.

FENWICK, E. M., MARTY, A. & NEHER, E. (1982). Sodium and calcium channels in bovine chromaffin cells. *Journal of Physiology* **331**, 599–635.

FINDLAY, I. (1987*a*). The effects of magnesium upon adenosine triphosphate-sensitive potassium channels in a rat insulin-secreting cell line. *Journal of Physiology* **391**, 611–629.

FINDLAY, I. (1987*b*). ATP-sensitive K^+ channels in rat ventricular myocytes are blocked and inactivated by internal divalent cations. *Pflügers Archiv* **410**, 313–320.

FINDLAY, I. (1988). Effects of ADP upon the ATP-sensitive K^+ channel in rat ventricular myocytes. *Journal of Membrane Biology* **101**, 83–92.

FINDLAY, I., DUNNE, J. M. & PETERSEN, O. H. (1985). ATP-sensitive inward rectifier and voltage- and calcium-activated K^+ channels in cultured pancreatic islet cells. *Journal of Membrane Biology* **88**, 165–172.

HAMILL, O. P., MARTY, A., NEHER, E., SAKMANN, B. & SIGWORTH, F. J. (1981). Improved patch-clamp techniques for high-resolution current recordings from cells and cell-free membrane patches. *Pflügers Archiv* **351**, 85–100.

HILLE, B. (1984). *Ionic Channels of Excitable Membrane*. Sinauer, Sunderland, MA, USA.

HIRANO, Y. & HIRAOKA, M. (1988). Barium-induced automatic activity in isolated ventricular myocytes from guinea-pig hearts. *Journal of Physiology* **395**, 455–472.

HORIE, M., IRISAWA, H. & NOMA, A. (1987). Voltage-dependent magnesium block of adenosine-triphosphate-sensitive potassium channels in guinea-pig ventricular cells. *Journal of Physiology* **387**, 251–272.

ISENBERG, G. & KLÖCKNER, U. (1982). Calcium-tolerant ventricular myocytes prepared by preincubation in a 'KB medium'. *Pflügers Archiv* **395**, 6–18.

KAKEI, M., KELLY, R. P., ASHCROFT, S. J. H. & ASHCROFT, F. M. (1986). The ATP-sensitivity of K^+ channels in rat pancreatic B-cells is modulated by ADP. *FEBS Letters* **208**, 63–66.

KAKEI, M. & NOMA, A. (1984). Adenosine-5′-triphosphate-sensitive single potassium channel in the atrioventricular node cell of the rabbit heart. *Journal of Physiology* **352**, 265–284.

KAKEI, M., NOMA, A. & SHIBASAKI, T. (1985). Properties of adenosine-triphosphate-regulated potassium channels in guinea-pig ventricular cells. *Journal of Physiology* **363**, 441–462.

LEDERER, W. J. & NICHOLS, C. G. (1989). Nucleotide modulation of the activity of rat heart ATP-sensitive K^+ channels in isolated membrane patches. *Journal of Physiology* **419**, 193–211.

NELDER, J. A. & MEAD, R. (1965). A simplex method for function minimization. *Computer Journal* **7**, 308–313.

NOMA, A. (1983). ATP-regulated K^+ channels in cardiac muscle. *Nature* **305**, 147–148.

PATLAK, J. & HORN, R. (1982). Effect of *N*-bromoacetamide on single sodium channel currents in excised membrane patches. *Journal of General Physiology* **79**, 333–351.

QIN, D., TAKANO, M. & NOMA, A. (1989). Kinetics of ATP-sensitive K^+ channel revealed with oil-gate concentration jump method. *American Journal of Physiology* **257**, H1624–1633.

QUAYLE, J. M., STANDEN, N. B. & STANFIELD, P. R. (1988). The voltage-dependent block of ATP-sensitive potassium channels of frog skeletal muscle by caesium and barium ions. *Journal of Physiology* **405**, 677–697.

RIBALET, B., CIANI, S. & EDDLESTONE, G. T. (1989). ATP mediates both activation and inhibition of K(ATP) channel activity via cAMP-dependent protein kinase in insulin-secreting cell lines. *Journal of General Physiology* **94**, 693–717.

RORSMAN, P. & TRUBE, G. (1985). Glucose-dependent K^+ channels in pancreatic B-cells are regulated by intracellular ATP. *Pflügers Archiv* **495**, 305–309.

SPRUCE, A. E., STANDEN, N. B. & STANFIELD, P. R. (1985). Voltage-dependent, ATP-sensitive potassium channels of skeletal muscle membrane. *Nature* **316**, 736–738.

SPRUCE, A. E., STANDEN, N. B. & STANFIELD, P. R. (1987). Studies of the unitary properties of adenosine-5′-triphosphate-regulated potassium channels of frog skeletal muscle. *Journal of Physiology* **382**, 213–236.

STANDEN, N. B., QUAYLE, J. M., DAVIES, N. W., BRAYDEN, J. E., HUANG, Y. & NELSON, M. T. (1989). Hyperpolarizing vasodilators activate ATP-sensitive K^+ channels in arterial smooth muscle. *Science* **245**, 177–180.

STANDEN, N. B., STANFIELD, P. R. & WARD, T. A. (1985). Properties of single potassium channels in vesicles formed from the sarcolemma of frog skeletal muscle. *Journal of Physiology* **364**, 339–358.

TAKANO, M., QIN, D. & NOMA, A. (1990). ATP-dependent decay and recovery of K^+ channels in guinea pig cardiac myocytes. *American Journal of Physiology* **258**, H45–50.

TRUBE, G. & HESCHELER, J. (1984). Inward-rectifying channels in isolated patches of the heart cell membrane: ATP-dependence and comparison with cell-attached patches. *Pflügers Archiv* **401**, 178–184.

ZILBERTER, Y., BERNASHEV, N., PAPIN, A., PORTNOV, V. & KHODOROV, B. (1988). Gating kinetics of ATP-sensitive single potassium channels in myocardial cells depends on electromotive force. *Pflügers Archiv* **411**, 584–589.